BLED WORKSHOPS
IN PHYSICS
VOL. 4, NO. 1

Proceedings of the Mini-Workshop
Effective q-q Interaction *(p. 107)*
Bled, Slovenia, July 7-14, 2003

Structure of the nucleon and the Δ from pion electro-production experiments at MAMI

S. Širca[a,b]

[a]Faculty of Mathematics and Physics, University of Ljubljana, 1000 Ljubljana, Slovenia
[b]Jožef Stefan Institute, 1000 Ljubljana, Slovenia

Abstract. Recent pion electro-production experiments of the A1 Collaboration at MAMI are presented. The threshold data in the $p(e,e'p)\pi^0$ and $d(e,e'd)\pi^0$ channels reveal the chiral dynamics of the pion-nucleon system at low energies. Measurements of the neutral channel in the Δ region address the issue of nucleon and/or Δ deformation and of the pion cloud, while the $p(e,e'\pi^+)n$ channel gives access to the axial structure of the nucleon.

1 Introduction

Electro-production of neutral or charged pions off nucleons close to the pion production threshold is an important tool to explore the structure of protons and neutrons at low energies. The s- and p-wave partial amplitudes in the $p\pi^0$ channel are bench-mark tests for predictions of the Chiral Perturbation Theory (ChiPT) which is believed to be a good low-energy approximation to QCD involving nucleon and pion degrees of freedom. Its validity can also be examined in the $n\pi^+$ channel which offers a possibility to extract the axial and induced pseudo-scalar form-factors of the proton. The threshold coherent π^0 production on the deuteron, used as an effective neutron target, is a sensitive probe of the chiral dynamics of the pion-neutron system. Experiments in the region of the Δ resonance probe the multipole structure of the $N \to \Delta$ transition by isolating interferences of small quadrupole transition amplitudes with the dominant magnetic dipole amplitude, and provide a quantitative measure for the deformation of the nucleon and/or the Δ. In addition, many observables in the $N \to \Delta$ transition exhibit large sensitivities to the effects of the pion cloud.

2 Testing ChiPT with $p(e,e'p)\pi^0$ and $d(e,e'd)\pi^0$ reactions

2.1 The proton

The first photo-production measurements $p(\gamma,p)\pi^0$ at threshold were designed to access the s-wave electric dipole amplitude E_{0+} [1] and thereby test the early low-energy theorems [2]. The severe disagreement between these theorems and the experiments was subsequently resolved by refined calculations in ChiPT [3], which also gave predictions for the p-wave multipole combinations P_i. Soon experimental work at MAMI extended to electro-production in order to study the

evolution of low-energy theorems of ChiPT [6]. In the first Mainz experiment at $Q^2 = 0.1\,(\mathrm{GeV/c})^2$, the s-wave amplitudes E_{0+} and L_{0+} were extracted by using *calculated* p-waves. In the transverse, longitudinal, and the interference terms in the cross-section, which can be decomposed by measuring the complete distributions in the azimuthal angle, the p-waves appear in specific combinations,

$$\begin{aligned}
P_1 &= 3E_{1+} + M_{1+} - M_{1-}\,,\\
P_2 &= 3E_{1+} - M_{1+} + M_{1-}\,,\\
P_3 &= 2M_{1+} + M_{1-}\,,\\
P_4 &= 4L_{1+} + L_{1-}\,,\\
P_5 &= L_{1-} - 2L_{1+}\,.
\end{aligned}$$

All multipoles are functions of the pion energy and of Q^2. Neglecting multipoles with $l \geq 2$, the structure functions can be expressed in terms of the multipoles as follows:

$$\begin{aligned}
R_T &= |\,E_{0+} + P_1 \cos\theta\,|^2 + \tfrac{1}{2}\big(|P_2|^2 + |P_3|^2\big)\,\sin^2\theta\,,\\
R_L &= |\,L_{0+} + P_4 \cos\theta\,|^2 + |\,P_5\,|^2\,\sin^2\theta\,,\\
R_{TL} &= -\sin\theta\,\mathrm{Re}\big[(E_{0+} + P_1\cos\theta)\,P_5^* + (L_{0+} + P_4\cos\theta)\,P_2^*\big]\,,\\
R_{TT} &= \tfrac{1}{2}\big(|\,P_2\,|^2 - |\,P_3\,|^2\big)\,\sin^2\theta\,,
\end{aligned} \tag{1}$$

where θ is the pion centre-of-mass angle.

For the experiment at $Q^2 = 0.1\,(\mathrm{GeV/c})^2$, the predictions for P_i were considered to be reliable because the one-pion-loop contributions are much smaller than those of the tree diagrams, contrary to the s-wave amplitudes E_{0+} and L_{0+} which pick up large pion-loop corrections even at threshold and at $Q^2 \to 0$. The low-energy parameters of ChiPT were fitted to the partial cross-sections of [5], and the photo-production data, the electro-production data, and the theory seemed consistent. However, the value of Q^2 was believed to be too high for the convergence of ChiPT.

Therefore, another experiment at $Q^2 = 0.05\,(\mathrm{GeV/c})^2$ was recently performed at MAMI [7], in which a model-independent extraction of the multipoles was attempted. Because the transverse-transverse interference term in the cross-section (1) was consistent with zero within the experimental uncertainty, only the s-wave multipoles and the combinations P_1, P_4, P_5 were extracted, while the P_2 and P_3 terms could not be separated: only their combination $P_{23} = \frac{1}{2}(|P_2|^2 + |P_3|^2)$ could be determined. The experiment showed large discrepancies with respect to the calculations. For example, the measured Q^2-dependence of the total cross-section, which is dominated by systematical uncertainties, strongly deviates from the prediction of ChiPT (see Fig. 1). Furthermore, there are large discrepancies between ChiPT and the MAID model [8]. Similar large disagreements were observed in the differential (and partial) cross-sections. While the resolution of the experiment was not good enough to perform a complete separation of the multipoles, it seems that the deviation is hidden in the P_{23} term which is constrained by photo-production and is not free to be re-adjusted to fit the new data set.

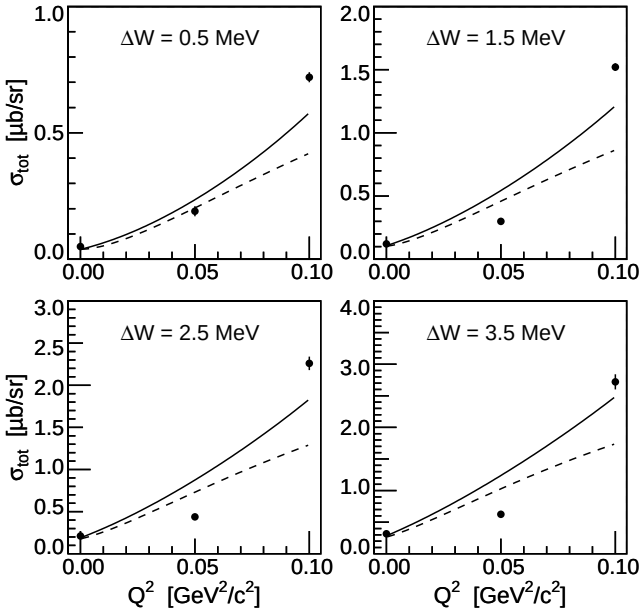

Fig. 1. The Q^2-dependence of the total cross-section for $p(e,e'p)\pi^0$ at four energies above threshold ΔW, at the virtual photon polarisation of $\varepsilon = 0.8$. The solid (dashed) curves are the prediction of ChiPT (MAID).

Since the discrepancy is large and seems to persist, this subject urgently needs further investigation. An experiment is planned at MAMI to scan the pertinent Q^2-region. Parts of the experimental programme have been performed in the Spring of 2003. An independent experiment, using the large-acceptance spectrometer BigBite, is being prepared at JLab [9] with extended kinematical coverage up to 20 MeV above threshold.

2.2 The deuteron

In the absence of free neutron targets, coherent π^0 electro-production from the deuteron has proven to be a promising way to obtain information on the electroproduction amplitude off a free neutron. In the impulse approximation, the full production amplitude is a coherent isoscalar sum of the free proton and neutron amplitudes. The nuclear binding effects are typically accounted for by means of deuteron form-factors. Interpreted in terms of ChiPT, the $d(e,e'd)\pi^0$ process establishes a connection to the pion-nucleon chiral dynamics in the proton channel: once the low-energy constants of ChiPT are optimally adjusted to describe the pion photo- and electro-production data sets on the proton, the measured deuteron threshold s-wave amplitudes E_d and L_d (analogs of E_{0+} and L_{0+} of the proton case) can be used to extract the predictions for the neutron amplitudes without introducing new or readjusting old low-energy parameters.

A cross-section measurement with real photons was performed at SAL, using coincidence detection of the π^0-decay photons in the IGLOO detector [10]. Since the missing-mass resolution was insufficient to separate the coherent channel from the deuteron breakup, the breakup contribution was subtracted by using a model, yielding $E_d = (-1.45 \pm 0.09) \times 10^{-3}/m_\pi$. This value is about 20% below the prediction of ChiPT, $E_d = (-1.8 \pm 0.6) \times 10^{-3}/m_\pi$ [11], but it is within the error bars.

The first experiment at finite Q^2 and close to threshold was recently performed at MAMI [12]. In this experiment, a magnetic spectrometer was used to detect the deuterons, thereby cleanly separating the coherent from the breakup channel. However, the detection of the low-energy deuterons suffering from large energy loss and multiple scattering, limited the Q^2 range to $0.1\,(\mathrm{GeV/c})^2$. The complete centre-of-mass solid angle was covered up to 4 MeV above threshold, and a Rosenbluth separation was performed. We extracted a value of $|L_d| = (0.50 \pm 0.11) \cdot 10^{-3}/m_\pi$ for the longitudinal s-wave amplitude at threshold, and an upper limit of $|E_d| \leq 0.42 \cdot 10^{-3}/m_\pi$. The results are shown in Fig. 2.

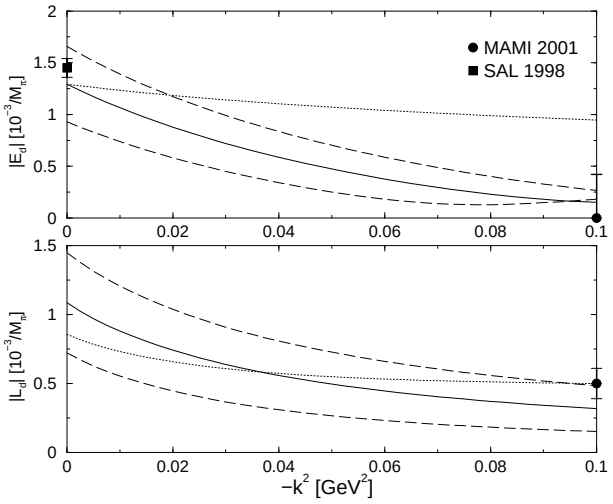

Fig. 2. The Q^2-dependence of the threshold s-wave multipoles E_d and L_d for $d(e,e'd)\pi^0$. The solid (dotted) curves represent fits 2 (1) of ChiPT (see [13] for details). The band between the dashed lines centered around fit 2 corresponds to a variation of the single-scattering amplitudes $E_{0+}^{(n)}$ and $L_{0+}^{(n)}$ by $\pm 1 \cdot 10^{-3}/m_\pi$.

The calculation of the threshold amplitude within ChiPT [13] showed that in order to understand the present data set, it is necessary to calculate the single-scattering (nucleon) amplitudes and three-body interactions in a consistent chiral scheme. A similar conclusion was reached in Ref. [14]. Since in the charged channel, the E_{0+} amplitude exceeds the one in the neutral channel by an order of magnitude (typically $|E_{0+}(n\pi^+)| \approx 20\,|E_{0+}(p\pi^0)|$), strong rescattering effects (involving pion loops) are anticipated, as illustrated in Fig. 3.

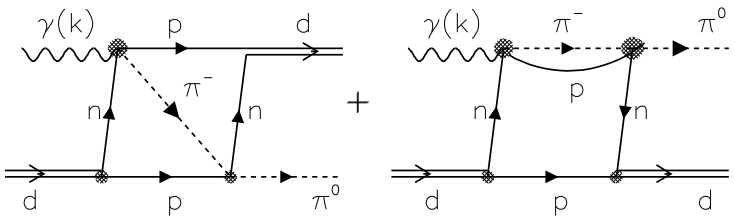

Fig. 3. Rescattering mechanisms in the $d(e,e'd)\pi^0$ process. (Figure adopted from [14].)

Considerations of rescattering effects in Ref. [14] show that it is most crucial to ensure proper anti-symmetrisation in the intermediate state, to apply correctly parity and angular momentum conservation, and to prevent double-counting. It was shown that rescattering effects cancel out, indicating that indeed the coherent π^0 production off the deuteron is a good way to access the elementary neutron amplitude. One of the observations supporting this conclusion is that also the unitary cusp observed in the $p\pi^0$ channel at the π^+ threshold disappears. However, the calculations in the framework of ChiPT also demonstrate that the p-wave multipoles are substantial and that the amplitudes possess a more complex momentum dependence than postulated in the original data analysis. Thus, even though consistency between data and theory seems to have been achieved (within the relatively large systematic uncertainties), more precise measurements at lower Q^2 would be beneficial to test these concepts accurately.

3 Nucleon axial and induced pseudo-scalar form-factors

Close to threshold, the transverse and longitudinal cross-sections for $p(e,e'\pi^+)n$ in parallel kinematics depend predominantly on the electric (E_{0+}) and the longitudinal (L_{0+}) multipoles, respectively. The E_{0+} amplitude is sensitive to the axial form-factor G_A, while the L_{0+} amplitude depends on the pion charge form-factor F_π and the induced pseudo-scalar form-factor G_P. Rosenbluth separations of the transverse and longitudinal cross-sections were performed in recent experiments at MAMI at an invariant mass of $W = 1125\,\mathrm{MeV}$ and several values of Q^2 (see Fig. 4 for kinematics coverage).

For the transverse cross-section, the s-wave dominance is known to persist to relatively high energies above the threshold. Thus the axial mass parameter M_A (a cut-off in the dipole parameterisation of G_A) has been extracted from the Q^2-dependence of transverse cross-section by using an effective Lagrangian model [15] in which G_A was the only adjustable form-factor while the electro-magnetic form-factors were assumed to be well-known.

One of the key difficulties in this extraction which directly translates into the variation in M_A is the value of the transverse cross-section in the real-photon limit. This value needs to be determined by extrapolation of angular distributions for photo-production $p(\gamma,\pi^+)n$ to zero, a procedure with a large systematical uncertainty (see Fig. 5).

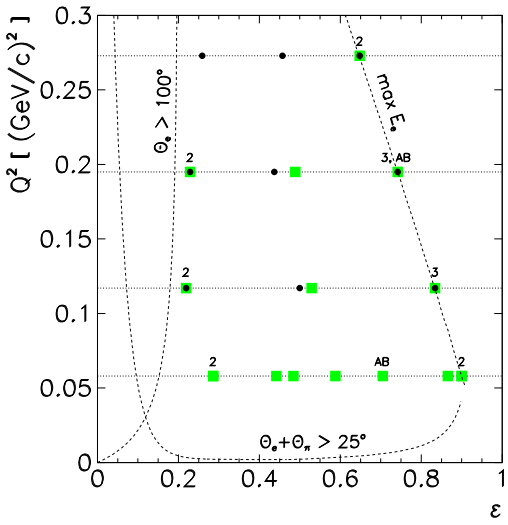

Fig. 4. Kinematics coverage for the Rosenbluth separations in the $p(e,e'\pi^+)n$ channel at $W = 1125\,\mathrm{MeV/c}$. Circles: published data [15]; squares: recently acquired data. The symbols '2' and '3' denote measurements repeated in different time periods, while 'AB' indicates spectrometer swaps which were performed to control systematics.

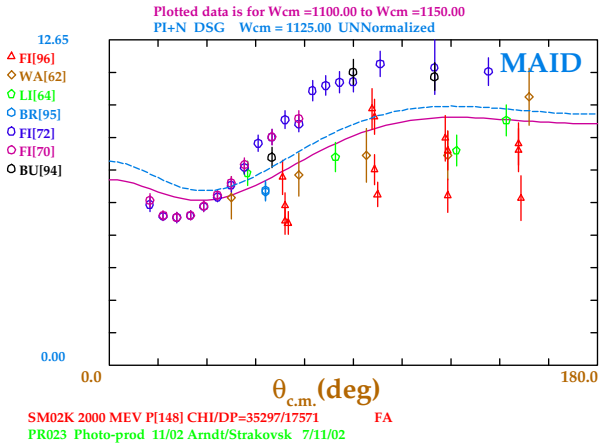

Fig. 5. Extrapolation of the photo-production angular distributions to zero in order to obtain the transverse cross-section at $Q^2 = 0$. The results of a partial-wave analysis SAID (full curve) and the Mainz Unitary Isobar Model MAID (dashed curve) are shown.

We have used a weighted-average cross-section at the photon point of $(7.22 \pm 0.36)\,\mu\mathrm{b/sr}$ (The corresponding value of $E_{0+}(n\pi^+)$ is also well supported by the studies of the GDH sum rule and by the low-energy (Kroll-Ruderman) limit.) The extracted value of $M_A = (1.077 \pm 0.039)\,\mathrm{GeV}$ is $(0.051 \pm 0.044)\,\mathrm{GeV}$ larger than the axial mass $M_A = (1.026 \pm 0.021)\,\mathrm{GeV}$ known from neutrino scattering

experiments. This 'axial mass discrepancy' is consistent with the prediction of ChiPT [16] which originates in pion-loop corrections to the electro-production process exemplified in Fig. 6.

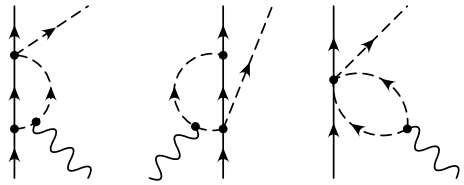

Fig. 6. Pion-loop corrections to the $p(e,e'\pi^+)n$ process which induce a modification of M_A. (Figure adopted from [16].)

Unfortunately, the kinematics range of the presently acquired data was too high for a direct application of the ChiPT result. The model-dependent terms, especially in the L_{0+} multipole, are of a size which does not allow to distinguish the pion form-factor from the induced pseudo-scalar form-factor. Even closer to threshold, however, also the longitudinal cross-section will be dominated by the s-wave, and we shall have

$$E_{0+}(q^2) = \frac{c}{\sqrt{2}f_\pi}\left[G_A(q^2) + \frac{q^2}{4M^2}\,G_A(0)G_M^v(q^2) + \cdots\right],$$
$$L_{0+}(q^2) = c\left[D(t) - 2MG_A(0)\right]\frac{\omega F_\pi(k_\pi^2)}{\sqrt{2}m_\pi f_\pi\,(2M+m_\pi)} + \frac{\omega}{m_\pi}\,E_{0+}(m_\pi^2)\,.$$

Here the divergence form-factor

$$D(t) = \frac{2f_\pi g_{\pi NN} m_\pi^2}{m_\pi^2 - t} + 2\left[MG_A(0) - f_\pi g_{\pi NN}\right]\frac{\lambda^2}{\lambda^2 - t}$$

measures the deviation of the induced pseudo-scalar form-factor G_P from its pion-pole dominance ($1/(m_\pi^2 - t)$) form. This allows one, by fitting λ to the data, a simultaneous extraction of G_A and G_P. To access very low Q^2 and pion momenta in the vicinity of the threshold, a dedicated short-orbit spectrometer is being commissioned in Mainz, and is expected to take data soon [17].

4 The N → Δ transition

One of the main goals of the $N \to \Delta$ experiments is to measure the Q^2-dependence of the transition amplitudes. The non-vanishing electric (E2) and Coulomb (C2) quadrupole amplitudes, which are much smaller than the leading magnetic dipole amplitude (M1), are an indication that the nucleon and/or the Δ deviate from spherical symmetry. Several mechanisms have been proposed to explain the nature of this deviation. In models involving explicit pion degrees of freedom, relatively large contributions to M1 and dominant contributions to E2 and

C2 originate in the coupling of the virtual photon to the p-wave pion field. The motivation behind the recent $N \to \Delta$ program at MAMI is to map out the M1, E2, and C2 multipoles in the region of low Q^2 where the pion-cloud effects are expected to play the most important role.

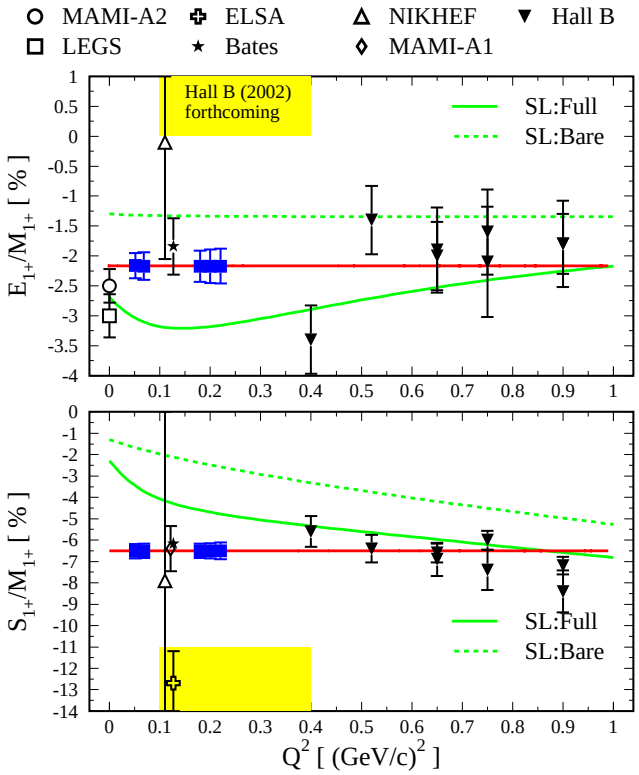

Fig. 7. Recent experimental data on the E2/M1 and C2/M1 ratios compared to the predictions of the model of Sato and Lee [18] (dashed curves: bare nucleon, full curves: including pion cloud) and MAID [8] (constant values of $-2.2\,\%$ and $-6.5\,\%$, respectively). The anticipated MAMI data (taken in the Spring of 2003) are shown with full squares.

The small quadrupole amplitudes E2 and C2 can be accessed through specific terms in the cross-section which contain interferences of the electro-production multipoles E_{1+} and S_{1+} with the dominant M_{1+}:

$$\begin{aligned}
\sigma_{0\pi}(\theta^\star_\pi) &= \sigma_0(\theta^\star_\pi) + \sigma_{TT}(\theta^\star_\pi) - \sigma_0(180^\circ) \\
&\sim 2\,(\cos\theta^\star_\pi + 1)\,\mathrm{Re}\,[E^*_{0+}M_{1+}] - 12\,\sin^2\theta^\star_\pi\,\mathrm{Re}\,[E^*_{1+}M_{1+}]\,, \\
\sigma_{LT}(\theta^\star_\pi) &\sim \sin\theta^\star_\pi\,\mathrm{Re}\,[S^*_{0+}M_{1+}] - 6\,\cos\theta^\star_\pi\,\sin\theta^\star_\pi\,\mathrm{Re}\,[S^*_{1+}M_{1+}]\,, \\
\sigma_{LT'}(\theta^\star_\pi) &\sim -\sin\theta^\star_\pi\,\mathrm{Im}\,[(-6\cos\theta^\star_\pi\,S_{1+} + S_{0+})^*M_{1+}]\,,
\end{aligned}$$

where θ^*_π is the emission angle of the pion in the centre-of-mass frame of the πN system and $\sigma_0 = \sigma_T + \varepsilon\sigma_L$. The $\sigma_{0\pi}$ and σ_{LT} terms exhibit large sensitivities to the E2/M1 ~ Re $[E^*_{1+}M_{1+}]$ and the C2/M1 ~ Re $[S^*_{1+}M_{1+}]$ ratios, respectively, while the $\sigma_{LT'}$ is sensitive to the imaginary part of the $S^*_{1+}M_{1+}$ interference.

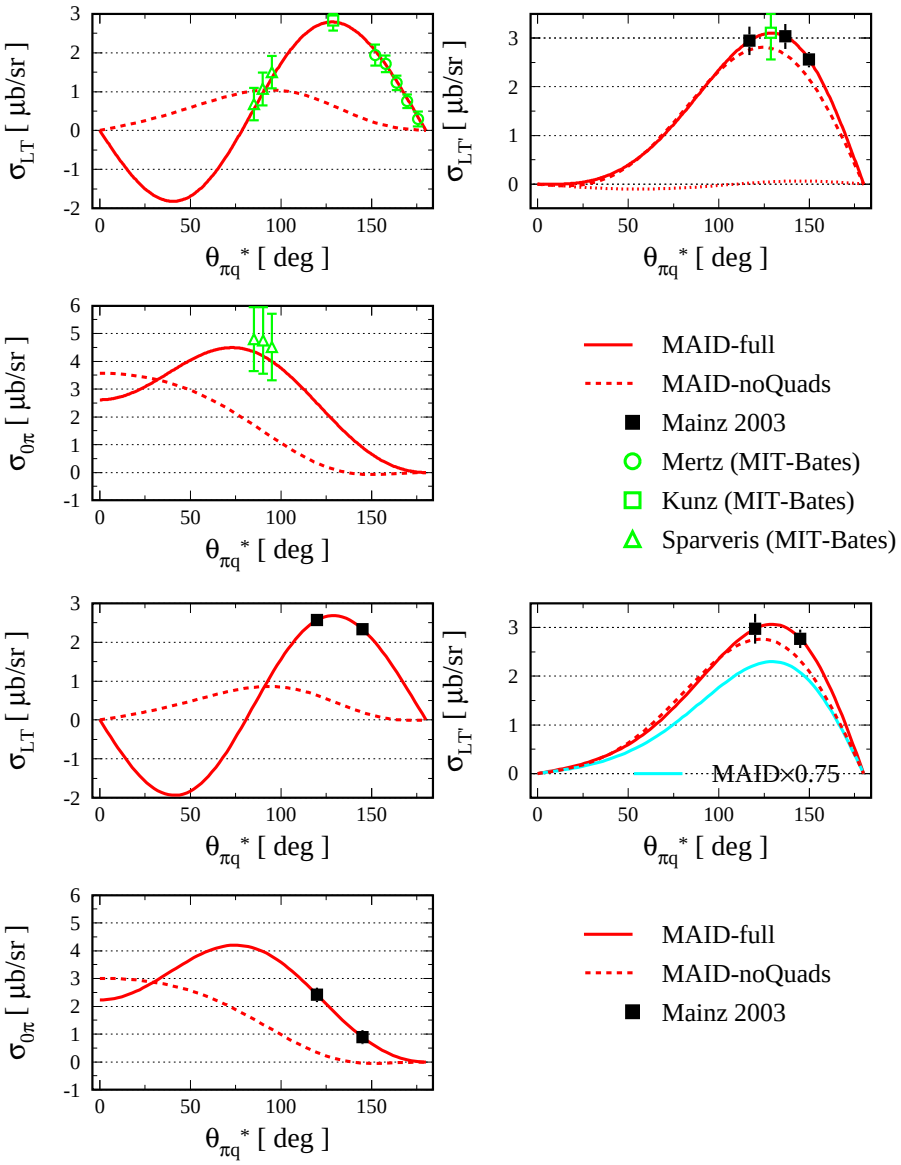

Fig. 8. Angular distributions of σ_{LT}, $\sigma_{LT'}$, and $\sigma_{\pi 0}$ for $Q^2 = 0.127$ (upper three panels) and 0.200 $(GeV/c)^2$ (lower three panels). The full curves indicate full MAID predictions, the dashed curves correspond to the MAID prediction without the quadrupole amplitudes. For details, see text.

In the Spring of 2003, new high-precision data in the $p(e,e'p)\pi^0$ channel were acquired at MAMI in the region of the Δ resonance, at four-momentum transfers of -0.06, -0.127, and $-0.2\,(\mathrm{GeV/c})^2$. The anticipated results for the E2/M1 and C2/M1 ratios as a function of Q^2 are shown in Fig. 7.

In addition to our primary goal, the extractions of E2/M1 and C2/M1 ratios at different Q^2, the present data set will try to answer several open questions arising from previous experiments at MIT-Bates and MAMI. For example, the measurement of $\sigma_{LT'}$ at $Q^2 = 0.2\,(\mathrm{GeV/c})^2$ will address the significant disagreement between MAID and the $A_{LT'}$ result from Mainz, which is underestimated by MAID by about 25 % [19]. The measurement of $\sigma_{LT'}$ at $Q^2 = 0.127\,(\mathrm{GeV/c})^2$ which overlaps with Bates will try to yield more insight into the apparent inability of the models to simultaneously describe the polarisation components obtained in the recoil-polarisation measurements [20]. At present, it is unclear where the violation of the consistency relation between P'_x, P'_z, and P^0_y comes from. The multipole structure of $\sigma_{LT'}$ resembles that of P^0_y, so we expect new data to help resolve this issue. The expected data points in the angular distributions of σ_{LT}, $\sigma_{LT'}$, and $\sigma_{0\pi}$ at $Q^2 = 0.127$ and $0.200\,(\mathrm{GeV/c})^2$ are shown in Fig. 8.

References

1. E. Mazzucato et al., Phys. Rev. Lett. **57** (1986) 3144;
   R. Beck et al., Phys. Rev. Lett. **65** (1990) 1841.
2. P. de Baenst, Nucl. Phys. B **24** (1970) 633;
   I.A. Vainshtein, V.I. Zakharov, Nucl. Phys. B **36** (1972) 589.
3. V. Bernard, N. Kaiser, J. Gasser, U.-G. Meißner, Phys. Lett. B **268** (1991) 291 (1991);
   V. Bernard et al., Nucl. Phys. B **383** (1992) 442;
   V. Bernard, N. Kaiser, U.-G. Meißner, Z. Phys. C **70** (1996) 483.
4. H.B. van den Brink et al., Phys. Rev. Lett. **74** (1995) 3561;
   T.P. Welch et al., Phys. Rev. Lett. **69** (1992) 2761.
5. M.O. Distler et al. (A1 Collaboration), Phys. Rev. Lett. **80** (1998) 2294.
6. V. Bernard, N. Kaiser, U.-G. Meißner, Nucl. Phys. A **607** (1996) 379;
   erratum ibid. **633** (1998) 695.
7. H. Merkel et al. (A1 Collaboration), Phys. Rev. Lett. **88** (2002) 012301.
8. D. Drechsel, O. Hanstein, S. S. Kamalov, L. Tiator, Nucl. Phys. A **645** (1999) 145.
9. R. Lindgren, D.W. Higinbotham, J.R.M Annand, V. Nelyubin (spokespersons), JLab Experiment E01–014.
10. J.C. Bergstrom et al., Phys. Rev. C **57** (1998) 3203.
11. S.R. Beane et al., Nucl. Phys. A **618** (1997) 381.
12. I. Ewald et al. (A1 Collaboration), Phys. Lett. B **499** (2001) 238.
13. H. Krebs, V. Bernard, U.-G. Meißner, Nucl. Phys. A **713** (2003) 405.
14. M.P. Rekalo, E. Tomasi-Gustafsson, Phys. Rev. C **66** (2002) 015203.
15. A. Liesenfeld, A.W. Richter, S. Širca et al. (A1 Collaboration), Phys. Lett. B **468** (1999) 20.
16. V. Bernard, L. Elouadrhiri, U.-G. Meißner, J. Phys. G: Nucl. Part. Phys. **28** (2002) R1.
17. R. Neuhausen (spokesperson), A1 Collaboration Proposal A1/1–98.
18. T. Sato, T.-S.H. Lee, Phys. Rev. C **63** (2001) 055201.
19. P. Bartsch et al. (A1 Collaboration), Phys. Rev. Lett. **88** (2002) 142001.
20. Th. Pospischil et al. (A1 Collaboration), Phys. Rev. Lett. **86** (2001) 2959.